Volume 9, Issue 10, October – 2024 International Journal of Innovative Science and Research Technology
ISSN No:-2456-2165 https://doi.org/10.38124/ijisrt/IJISRT24OCT336

# Optimization of the Thermokinetic Method for the Control of Weld Decay in AISI 304L and AISI 316L Stainless Steel Weldment

[1]O. G. Utu; [2]P. N. Atanmo; [3]I. U. Onyenanu; [4]K. C. Owauma; [5]P. A. Olubambi
[1]Department of Welding and Fabrication Engineering Technology, Delta State Polytechnic Ogwashi Uku Delta State.
[2,3,4]Department of Mechanical Engineering, Chukwuemeka Ojukwu Odumegwu University, Uli Anambra State.
[5]Department of Metallurgy and Chemical Engineering, University of Johannesburg, South Africa.

**Abstract:- This study investigates the control of weld decay in AISI 304L/316L alloy weldments for liquefied natural gas (LNG) and cryogenic environments using the Tungsten Inert Gas (TIG) welding technique. Weldment samples were thermokinetically treated at 1050, 1100, and 1150°C and cooled in five mediums: Water, Salt, Natural Air, Salt with annealing, and Water with annealing, to retain carbon and chromium in solid solution at approximately 30°C. Furthermore, evaluation methods based on metallography i.e. optical microscopy (OM), Scanning Electron Microscopy (SEM) and Energy Dispersive X-Ray Spectroscopy (EDX), Wear Test (i.e. wear rate and wear track) and electrochemical corrosion potential measurements were adopted. An experimental design table was developed using the design expert software 13.0. This helped develop a predictive mathematical model for ascertaining the optimum operating service conditions of the material. From the results, the optical microscopy analysis revealed that the control sample exhibited a more irregular pattern than others. Results showed that the control sample had a more irregular structure, while air-cooled samples exhibited smoother surfaces, indicating better bonding. SEM revealed a coarse surface with uneven particle distribution post-heat application. The predominant elements were Iron (Fe), Chromium (Cr), and Nickel (Ni). Corrosion potential varied between -0.5 to 0.15 V, demonstrating wave-like behaviour over time. Wear analysis indicated that lower coefficients of friction correlate with better wear resistance. Finally, response surface methodology (RSM) revealed that increasing temperature proportionally increased yield and corrosion rates. While the identified optimal values for Temperature are (1112.68°C), Material (316L), and Quenching Medium (SQ+SA), resulting in specific values such as Wear Rate (5.76896E-06), Coefficient of friction (0.224254), Corrosion Rate (0.395566), and Weight of Heat-Treated Sample (14.7797). The study enhances understanding of the mechanisms affecting welding and contributes to optimizing welding procedures for improved mechanical properties and corrosion resistance.**

## I. INTRODUCTION

Corrosion is a major cause of weldment failures even after welding the base metal with the proper filler metal, adhering to the right industry codes and standards, and having a sound weld. The wrought form of a metal or an alloy can resist corrosion in a particular environment but the welded counterpart will not. In other instances, the weld can exhibit corrosion resistance superior to the un-welded base metal depending on the variation in composition and metallurgical properties. Weld decay is a significant concern in industries where stainless steels are used in corrosive environments, such as chemical processing, marine applications, and nuclear power plants [1]. This form of intergranular corrosion occurs due to chromium depletion along grain boundaries, which makes the welded regions more susceptible to corrosive attack. This can lead to a reduction in the strength, toughness, and service life of welded components, especially in aggressive environments. Understanding and mitigating weld decay is crucial for ensuring welded stainless-steel structures' long-term integrity and safety [2]

Austenitic stainless steels are iron-based alloys with at least 16% chromium and sufficient nickel or manganese to maintain an austenitic structure across all temperatures [3]. Among grades, 316 stainless steel typically offers better resistance to weld decay due to its molybdenum content. These alloys are widely utilized in steam-generating plants, chemical reactors, and nuclear facilities because of their excellent corrosion resistance and good mechanical properties.

However, when exposed to welding temperatures between 500°C and 800°C, they can suffer from intergranular corrosion and stress corrosion cracking, primarily due to sensitization from chromium depletion along grain boundaries [4], [5]. This depletion results from carbide formation, specifically Cr23C6, influenced by carbon content, temperature, and exposure duration [6], [7].

Light gauge steel typically avoids these issues due to rapid cooling post-welding [8]. Solidification and liquation cracking can also occur, necessitating careful selection of filler metals to minimize susceptibility [9]. The degree of sensitization is significantly affected by grain size and boundary characteristics [10].

ISSN No:-2456-2165 https://doi.org/10.38124/ijisrt/IJISRT24OCT336

Furthermore, research concerning grain boundary architecture and manipulation has indicated that materials exhibiting a high prevalence of low-energy grain boundaries, such as coincidence site lattice boundaries, demonstrate considerable resistance to intergranular precipitation and corrosion [11], [12]. Additionally, it has been documented that the DOS is inversely correlated with grain size and exhibits a nearly exponential decline as grain boundary surface area increases (which corresponds to a decrease in grain size) [13]. The thermokinetic approach signifies a considerable progression in the management of weld decay in AISI 304L and 316L stainless steel weldments. Through the meticulous regulation of the thermal history within the heat-affected zone, this method provides a formidable instrument for the enhancement of corrosion resistance and mechanical characteristics of welded joints. Although obstacles persist regarding process regulation, equipment expenditures, and requisite expertise, the advantages of the thermokinetic method are unequivocal. Its capacity to alleviate sensitization and enhance overall weld integrity renders it an indispensable technique in sectors where the reliability of stainless-steel welds is paramount.

The thermokinetic approach to managing weld decay focuses on controlling the time-temperature relationship during and after welding to minimize sensitization. Techniques include controlled cooling rates, post-weld heat treatment (PWHT), and in-situ monitoring systems. These methods aim to manage carbide formation and chromium diffusion, thereby reducing the risk of sensitization [14], [15].

Controlled cooling rates can significantly reduce the time for carbide precipitation, while thermal cycling can promote carbide dissolution. Advanced monitoring techniques enable real-time adjustments during welding, which helps minimize exposure to sensitization temperatures [16]. The effectiveness of the thermokinetic method in controlling weld decay has been demonstrated through various studies. Research by Vasudevan et al., (2003) showed that optimized cooling rates could reduce the degree of sensitization in 304 stainless steel welds by up to 80% compared to air-cooled samples. Similarly, work by Zeng et al., (2021) on 316 stainless steel revealed that controlled thermal cycling could effectively restore chromium distribution in sensitized regions, significantly improving corrosion resistance. However, implementing thermokinetic control methods in industrial settings can present challenges, including the need for specialized equipment, potential difficulties with complex geometries, and the requirement for precise control over a wide range of process parameters [17].

Despite these challenges, the thermokinetic approach offers significant potential for improving the integrity of austenitic stainless steel welds. Ongoing research in this field is focused on developing more sophisticated modelling techniques to predict sensitization behaviour, integrating artificial intelligence for real-time process optimization, and exploring novel cooling methods for enhanced control over thermal profiles [18]. As our understanding of the thermokinetics of weld decay continues to evolve, this work intends to appraise the control of weld decay in AISI 304L / 316L stainless steel weldment using the thermokinetic method.

## II. AIM AND OBJECTIVES OF THE STUDY

This work is aimed at investigating the thermokinetic method for the control of weld decay in AISI 304L / 316L stainless steel weldment. Hence, the specific objectives are to;

- Determine the optimum heat treatment temperature for thermokinetic processing of the weldments, then allow an optimum soaking time to achieve desensitization of the weldments.
- Expose the heat-treated samples to various quenchants (water, natural air, salt, salt with annealing and water with annealing) required to rapidly cool the weldments from the optimum heating temperature to room temperature (about $33^0$C) and thus ensure the weldments remain desensitized.
- Examine the samples' microstructure using Optical Microscopy (OM), Scanning Electron Microscopy (SEM) and Energy dispersal X-ray spectrometry (EDX). Then, conduct a wear test (i.e. wear rate and wear track) and later expose the samples to 0.3m $H_2SO_4$ and NaCl solution to determine corrosion penetration using the Potentio dynamic polarization method to determine corrosion rate.
- Optimize the results generated using the optimal custom approach in Response Surface Methodology (RSM) in other to create a thermokinetic model that accurately predicts the susceptibility of weldments to decay based on various welding parameters.
- Validate the models using experimental data in other to determine optimal welding parameters that minimize weld decay.

However, the study seeks to contribute to the advancement of welding technology and improve the performance of critical components in industries such as petrochemical, marine, and food processing. It will further help in solving weld decay (intergranular corrosion) problems in welded austenitic stainless-steel types AISI 304L/316L used in transmission pipelines, silos, food storage equipment, flow lines, oil drilling tubular in the hydrocarbon industries and also in other major sectors such building construction, manufacturing, and transportation, etc.

Volume 9, Issue 10, October – 2024 International Journal of Innovative Science and Research Technology
ISSN No:-2456-2165 https://doi.org/10.38124/ijisrt/IJISRT24OCT336

## III. METHODOLOGY

### A. *The Process Flow Diagram*

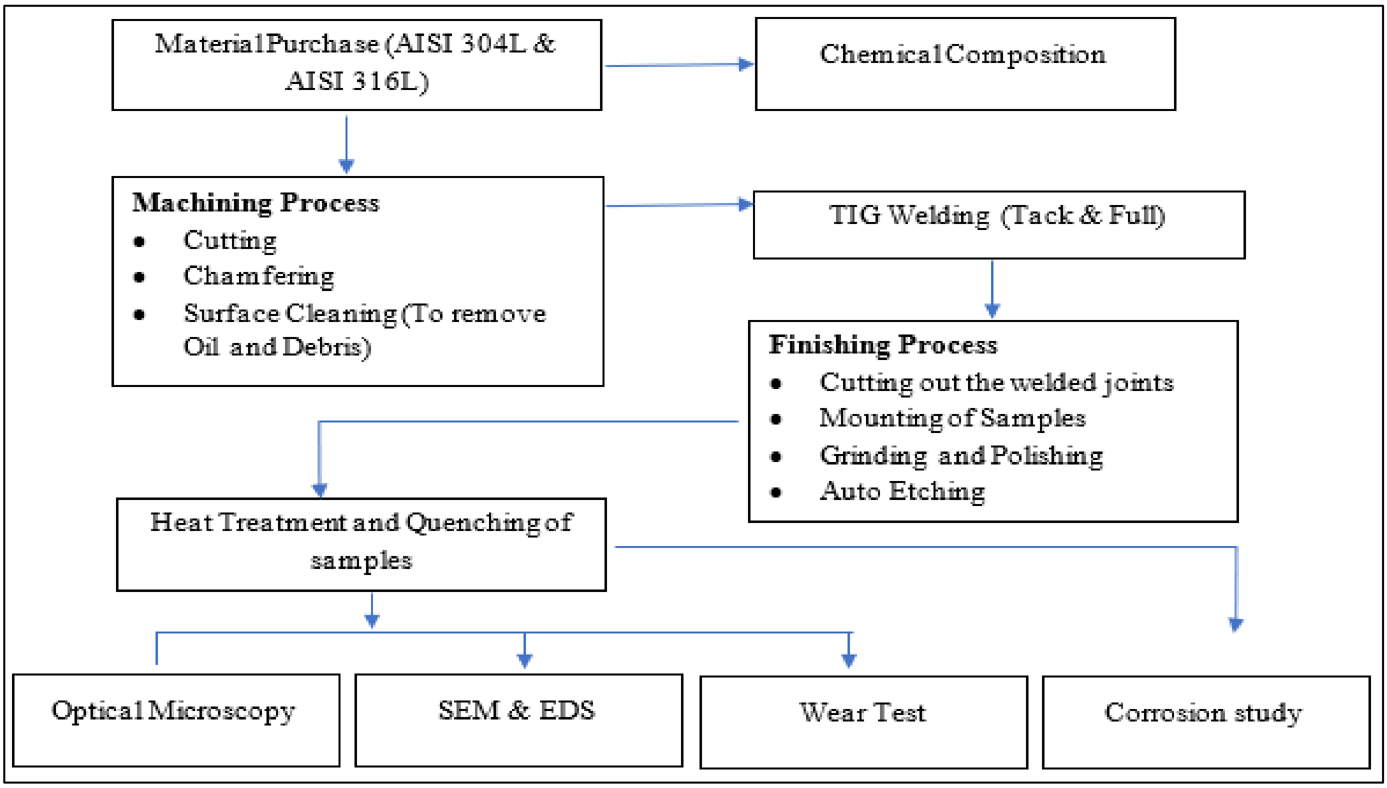


Fig 1: Detailed Approach to the Study

### B. *Materials and Equipment*

➢ *Materials*

The materials used for this study are the typical AISI type 304L and 316L stainless steel. Table 1 shows the nominal elemental compositions of typical AISI-type 304L and 316L stainless steel.

Table 1: Nominal Chemical Compositions of Typical AISI Type 304L and 316L Stainless Steel

| **Element** | **AISI 304L Stainless Steel Material (% by wt.)** | **AISI 316L Stainless Steel Material (% by wt.)** |
|---|---|---|
| Carbon (C) | 0.03 | 0.03 |
| Chromium (Cr) | 19.0 | 16.50 |
| Nickel (Ni) | 10 | 11 |
| Manganese (Mn) | 2.00 | 2.00 |
| Silicon (Si) | 1.00 | 1.00 |
| Molybdenum (Mo) | 0.00 | 3.00 |
| Phosphorus (P) | 0.040 | 0.03 |
| Sulphur (S) | 0.035 | 0.035 |
| Iron (Fe) | Remainder | Remainder |

Source: [19]

Other materials include etchant (hydrochloric acid reagent and iron chloride), ER308L filler material, ER316L filler material, distilled water, and saline water.

➢ *Equipment:*

Metal Tong, desiccator, furnace tray, digital weighing machine, face mask, surgical glove, flow meter, measuring tape, plastic pouch bag, stainless wire brush, PMI Oxford instruments, centre lathe machine, SEM/EDX, TIG welding machine, argon gas, automatic grinding and polishing machine, Tribometer, furnace, EDM Wire cutting machine, hot mounting press and auto-etching machine.

### C. *Methods*

➢ *Sample Collection*

The sample types AISI304L/316L stainless steel flat bar were purchased from Turret Engineering Services Port-Harcourt, Rivers State. The chemical composition of the materials was determined using PM/Oxford Instrument by Turret Engineering Services.

➢ *Sample Preparation*

Each material type (AISI 3034L/ AISI 316L) flat bar was prepared by cutting into forty-four (44) pieces of 25mm x 25mm x 10mm. The cut pieces were paired into butt-weld single V-groove joints and welded by a tungsten inert gas (TIG) process. Twenty-two (22) welded pairs were produced. After the welding operation, the welded samples welded zone were cut off from the main material measuring 10mm x 10mm x 3mm. Depending on the availability of prequalified welders (skilled welders). The welders were tested/ prequalified on the American Welding Society (AWS)

ISSN No:-2456-2165 https://doi.org/10.38124/ijisrt/IJISRT24OCT336

procedure. This is to eliminate limitations in workmanship. All welds were made with stainless steel (SS) filler rods containing carbon % by mass fraction compatible with that of base metal (0.028% for 304L and 0.031% for 316L). The weldment was free-air cooled. The welding procedure specification was referenced to AWS B2.1: Standard for welding procedure and performance Qualification, being one of the reference standards for welding procedure specifications.

The welded samples used for the research work were chemically cleaned by immersions and in the process, the native oxides were removed. This native oxide, are the initial oxides of Cr formed as a protective layer. These are considered to inhibit the diffusion of elements in the matrix. Heat input rate was determined before heating. All the welded specimens were prepared and thermo-kinetically treated (temperature input variable and quenching variable) in a furnace with a protective environment as follows:

*D. Experimental Design Table*

The below table shows the sample behaviours without heat treatment, under different heat treatment which includes salt quench, water quenched and air cooling, the different mean values, wear rate and corrosion rate at every sample in a specified temperature range testing were presented in this table below.

Table 2: Samples' Behaviour on Heat Treatment

| **Samples** | **Description** | **Mean C °F @ 10N Load** | **Wear Rate ($mm^3/mN$)** | **Corrosion rate mm/year in $H_2SO_4$** | **Weight (g)** |
|---|---|---|---|---|---|
| 19 | **Control (304 without treatment)** | | | | |
| | 304 stainless steel heat treated at 1050 degrees | | | | |
| 4 | Salt Quenched | | | | |
| 3 | Water Quenched | | | | |
| 13 | Air Cooled | | | | |
| 29 | Salt Quenched + Annealing | | | | |
| 27 | Water Quenched + Annealing | | | | |
| | 304 stainless steel heat treated at 1100 degrees | | | | |
| | Salt Quenched | | | | |
| | Water Quenched | | | | |
| | Air Cooled | | | | |
| | Salt Quenched + Annealing | | | | |
| | Water Quenched + Annealing | | | | |
| | Control | | | | |
| | 304 stainless steel heat treated at 1150 degrees | | | | |
| 21 | Salt Quenched | | | | |
| 16 | Water Quenched | | | | |
| 25 | Air Cooled | | | | |
| 11 | Salt Quenched + Annealing | | | | |
| 10 | Water Quenched + Annealing | | | | |
| | | | | | |
| 19 | **Control (316 without treatment)** | | | | |
| | 316 stainless steel heat treated at 1050 degrees | | | | |
| 02 | Salt Quenched | | | | |
| 05 | Water Quenched | | | | |
| 01 | Air Cooled | | | | |
| 28 | Salt Quenched + Annealing | | | | |
| 31 | Water Quenched + Annealing | | | | |
| 20 | Control | | | | |
| | 316 stainless steel heat treated at 1100 degrees | | | | |
| | Salt Quenched | | | | |
| | Water Quenched | | | | |
| | Air Cooled | | | | |
| | Salt Quenched + Annealing | | | | |
| | Water Quenched + Annealing | | | | |
| 20 | Control | | | | |
| | 316 stainless steel heat treated at 1150 degrees | | | | |
| 18 | Salt Quenched | | | | |
| 24 | Water Quenched | | | | |
| 14 | Air Cooled | | | | |

ISSN No:-2456-2165 https://doi.org/10.38124/ijisrt/IJISRT24OCT336

| | | | | | |
|---|---|---|---|---|---|
| 30 | Salt Quenched + Annealing | | | | |
| 7 | Water Quenched + Annealing | | | | |
| 20 | Control | | | | |

## IV. RESULTS AND DISCUSSION

### *A. Optical Microscopy Result*

Figure 1 illustrates the optical micrograph depicting the microstructure of 316L austenitic stainless steel heated to 1050 °C at 10 magnification, serving as the reference sample in the study.

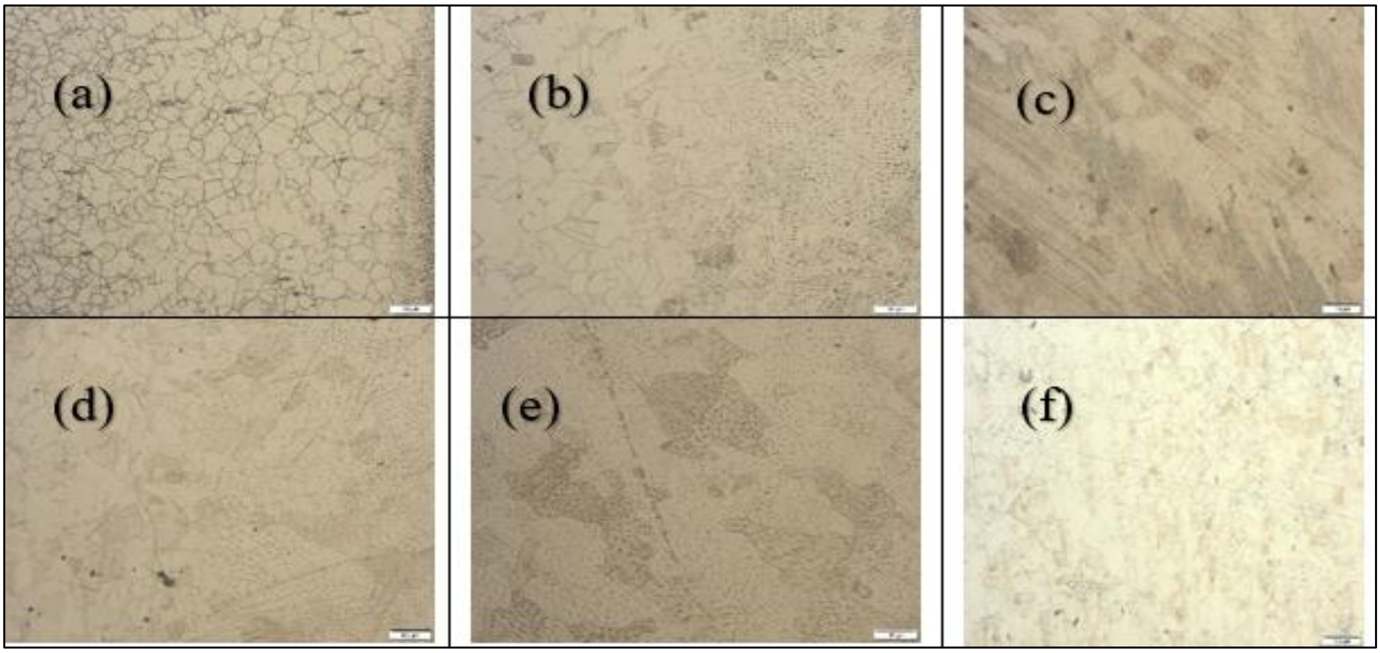


Fig 2: Optical Microscopy Results for 316L Austenitic Stainless Steel 1050 °C (a) Control Sample (b) Salt Quenched (c) Water Quenched (d) Air-Cooled (e) Salt Quenched Followed by Annealing (f) Water Quenched Followed by Annealing

### *B. Scanning Electron Microscopy and EDX*

Scanning Electron Microscopy (SEM) was utilized to analyze the surface morphology of the (WJ, HAZ, and PM) welded joint, heat affected area, and the parent materials.

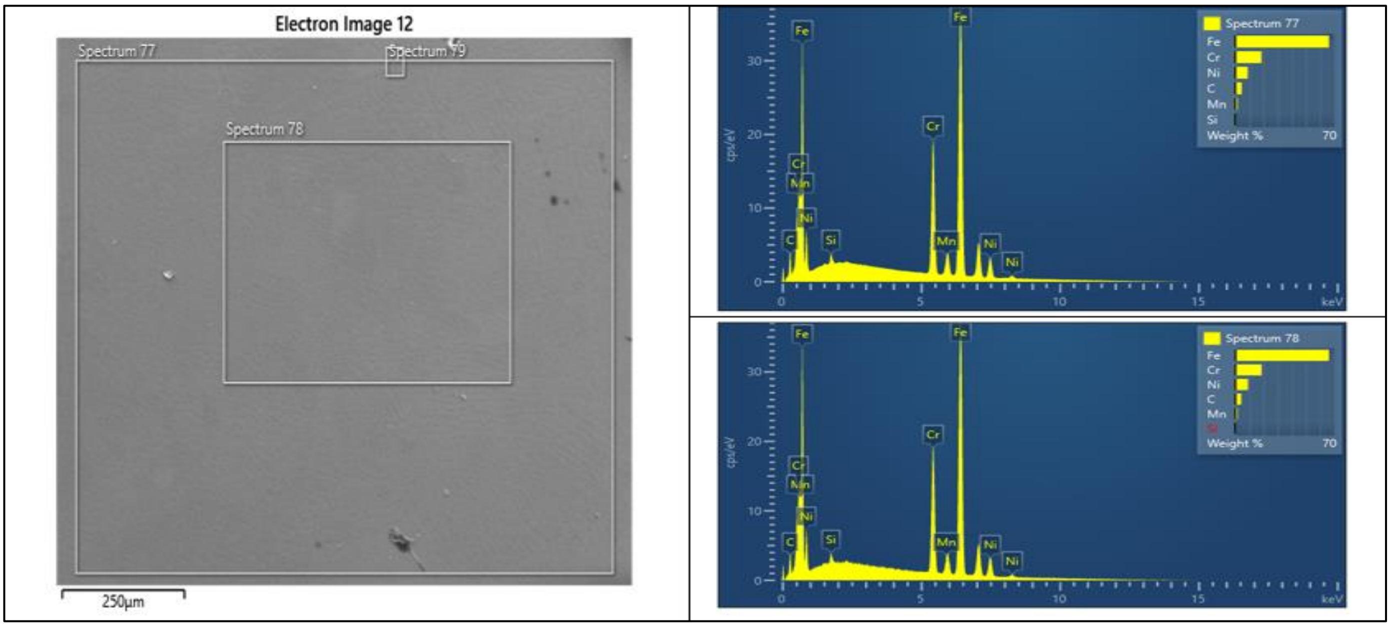


Fig 3: SEM Result and EDX Analysis of 304L Stainless Heat Treated at 1050°C and Quenched in Water

ISSN No:-2456-2165 https://doi.org/10.38124/ijisrt/IJISRT24OCT336

### *C. Wear and Coefficient of Friction (COF) Result*

The coefficient of friction (COF) is significant in wear tests. It provides insights into the frictional behavior of materials, Influencing wear rates, energy efficiency, and material performance.

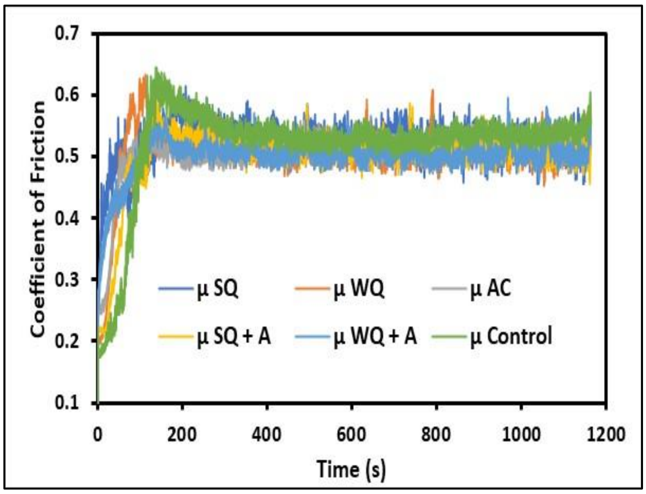


Fig 4(a): Variation in Coefficient of Friction for 304L Austenitic Stainless Steel Heat Treated at 1050ºC Subjected to 10 N Load

### *D. Corrosion Rate Results*

Corrosion is the gradual degradation of materials, often metals, due to chemical reactions with their environment. In electrochemical systems, cathodes are critical components that can be prone to corrosion, impacting the system's performance and longevity. Heat treatment is commonly used to alter the microstructure of cathodes, potentially improving their corrosion resistance. For this research, different quench mediums after heat treatment were considered including water, air, and salt quenching others include the water quench in addition to annealing, and the salt quench in addition to annealing. From the graph, $E_0$(Ag/AgCl) is represented at the y-axis for each heat treatment temperature while the current and time are represented on (the x-axis) respectively.

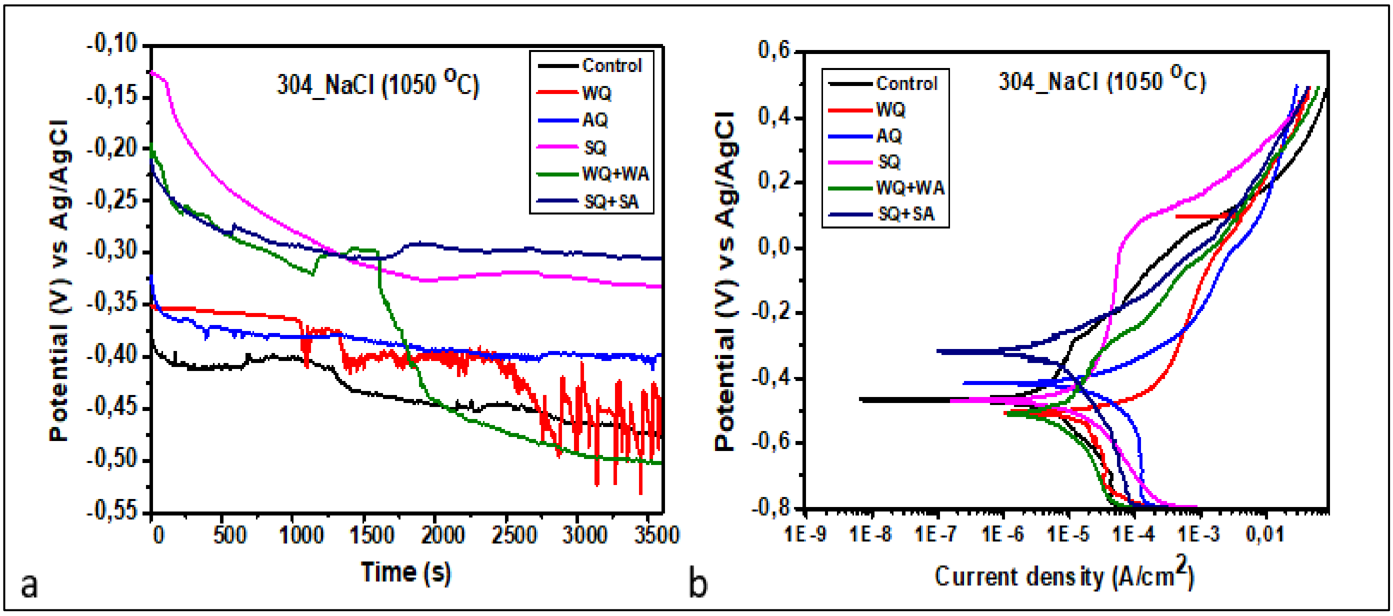


Fig 5: Graph of E0(Ag/AgCl) against Time (s) at Temperature 1050℃ of 304L

### *E. Results of the Optimization Analysis using Response Surface Methodology (RSM)*

Preliminary study on the control of weld decay problem in AISI types 304L and 316L SS weldments using thermokinetic approach. Four excipients were chosen for the optimized responses these factors include the temperature change, material, quenching medium, and wear rate as they may affect the responses. The ranges of variables were also studied by using a D-optimal mixture in design expert software. Table 3 shows the summary data table of the actual design after the experiment.

ISSN No:-2456-2165 https://doi.org/10.38124/ijisrt/IJISRT24OCT336

Table 3: Summary of the Actual Design Table for the optimization

| | Factor 1 | Factor 2 | Factor 3 | Response 1 | Response 2 | Response 3 | Response 4 |
|---|---|---|---|---|---|---|---|
| Run | A: Temperature (Deg. Celsius) | B: Material | C: Quenching Medium | Wear Rate ($mm^3/mN$) | Coefficient of Friction (CoF) | Corrosion Rate (mm/year) | Weight of Heat-Treated Samples (g) |
| 1 | 1050 | 304L | WQ+WA | 6.086E-06 | 0.501 | 0.2113 | 17.771 |
| 2 | 1100 | 316L | WQ+WA | 6.8012E-06 | 0.52 | 0.2587 | 15.0294 |
| 3 | 1150 | 316L | SQ+SA | 5.5648E-06 | 0.533 | 0.3119 | 14.0115 |
| 4 | 1100 | 316L | SQ | 6.3214E-06 | 0.38 | 1.7049 | 15.1247 |
| 5 | 1100 | 304L | SQ+SA | 4.7766E-06 | 0.504 | 0.2712 | 15.3278 |
| 6 | 1150 | 316L | AQ | 1.0781E-05 | 0.515 | 0.6817 | 14.0183 |
| 7 | 1150 | 304L | WQ+WA | 5.217E-06 | 0.53 | 0.2323 | 13.6796 |
| 8 | 1050 | 316L | SQ+SA | 6.0865E-06 | 0.58 | 0.3138 | 15.9547 |
| 9 | 1150 | 304L | SQ+SA | 4.3475E-06 | 0.506 | 0.2894 | 14.7244 |
| 10 | 1050 | 304L | AQ | 1.043E-05 | 0.506 | 0.3125 | 13.9566 |
| 11 | 1150 | 304L | WQ | 8.3472E-06 | 0.49 | 1.3773 | 13.1359 |
| 12 | 1100 | 304L | SQ | 6.4726E-06 | 0.51 | 1.2338 | 13.892 |
| 13 | 1100 | 304L | SQ | 6.4726E-06 | 0.51 | 1.2338 | 13.892 |
| 14 | 1100 | 304L | AQ | 9.5422E-06 | 0.508 | 0.4982 | 14.4702 |
| 15 | 1100 | 304L | AQ | 9.5422E-06 | 0.508 | 0.4982 | 14.4702 |
| 16 | 1050 | 304L | SQ | 6.956E-06 | 0.5 | 1.0572 | 15.1384 |
| 17 | 1100 | 316L | WQ+WA | 6.8012E-06 | 0.52 | 0.2587 | 15.0294 |
| 18 | 1100 | 316L | WQ | 8.5023E-06 | 0.512 | 1.4103 | 13.0483 |
| 19 | 1150 | 316L | SQ | 6.0865E-06 | 0.53 | 1.529 | 14.8997 |
| 20 | 1150 | 316L | WQ | 8.3472E-06 | 0.533 | 1.4513 | 13.0337 |
| 21 | 1050 | 316L | WQ | 8.695E-06 | 0.47 | 1.3817 | 14.492 |
| 22 | 1100 | 304L | WQ | 8.5124E-06 | 0.501 | 1.2243 | 14.2813 |
| 23 | 1100 | 304L | SQ+SA | 4.7766E-06 | 0.504 | 0.2712 | 15.3278 |
| 24 | 1100 | 304L | WQ+WA | 5.6204E-06 | 0.521 | 0.2413 | 15.7614 |
| 25 | 1050 | 316L | AQ | 1.026E-05 | 0.49 | 0.6524 | 13.8861 |
| 26 | 1050 | 304L | WQ | 8.695E-06 | 0.503 | 1.4442 | 16.1805 |
| 27 | 1100 | 316L | SQ | 6.3214E-06 | 0.38 | 1.7049 | 15.1247 |

➤ *Predicted and Actual Results for the three (4) Responses*

- *Wear Rate*

Utilizing the design expert software, optimization was conducted on the experimental design table. The coded equations were generated on each case and utilized to calculate the predicted values of the experiment. Fig. 6 shows the graphical representation of the predicted and actual values of the experiment. The graph confirms a high similarity between the predicted and actual values for the wear rate experiment.

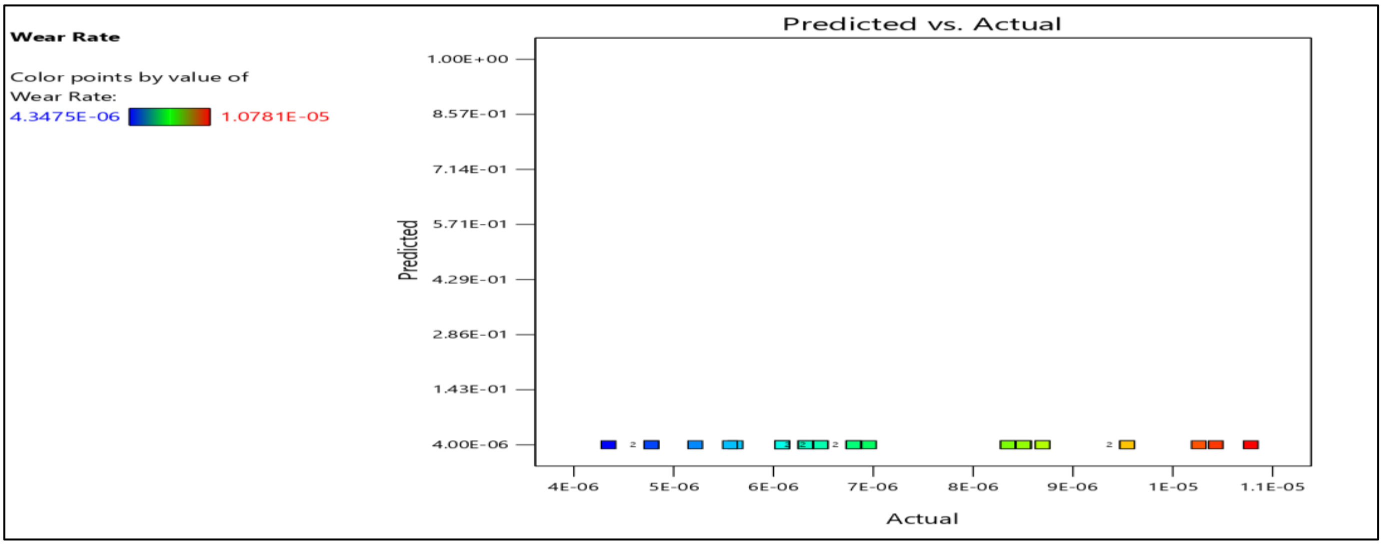


Fig 6: Showing the Predicted and Actual Values for the Wear Rate

ISSN No:-2456-2165 https://doi.org/10.38124/ijisrt/IJISRT24OCT336

- *Coefficient of Friction (CoF)*

Fig. 7 shows the graphical representation of the predicted and actual values of the Coefficient of Friction (CoF). Again, the graph confirms a high similarity between the predicted and actual values for the wear rate experiment.

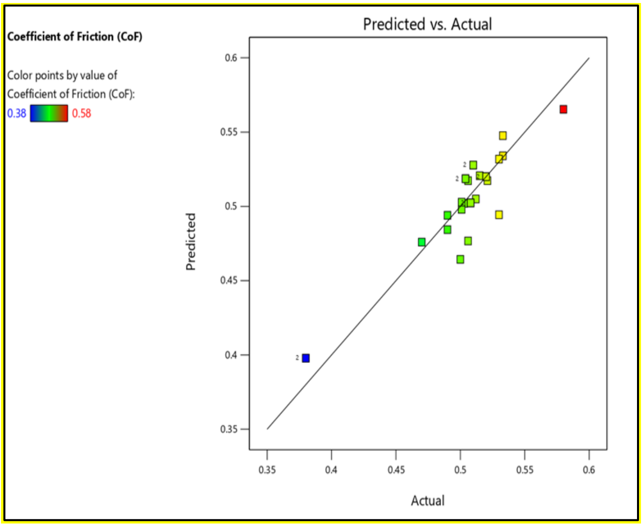


Fig 7: Showing the Predicted and Actual Values for the Coefficient of Friction (CoF).

- *Corrosion Rate*

Fig. 8 shows the graphical representation of the predicted and actual values of the corrosion Rate**.** Again, the graph confirms a high similarity between the predicted and actual values for the wear rate experiment.

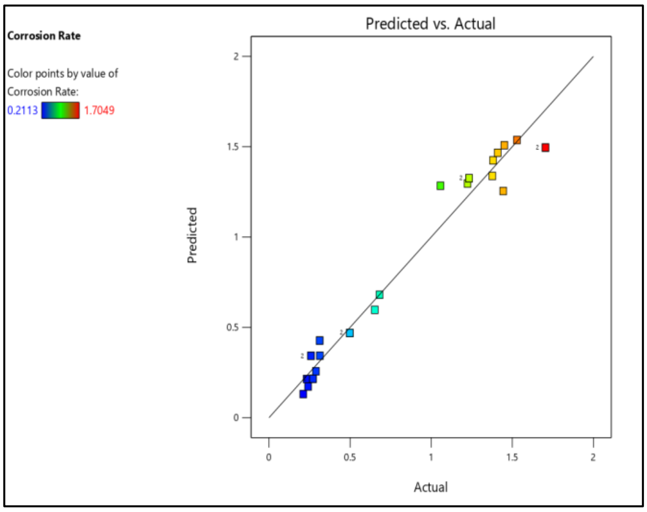


Fig 8: Showing the Predicted and Actual Values for the Corrosion Rate

- *Weight of Heat-Treated Samples*

Fig. 9 shows the graphical representation of the predicted and actual values of the **Weight of Heat**. Again, the graph confirms a high similarity between the predicted and actual values for the wear rate experiment.

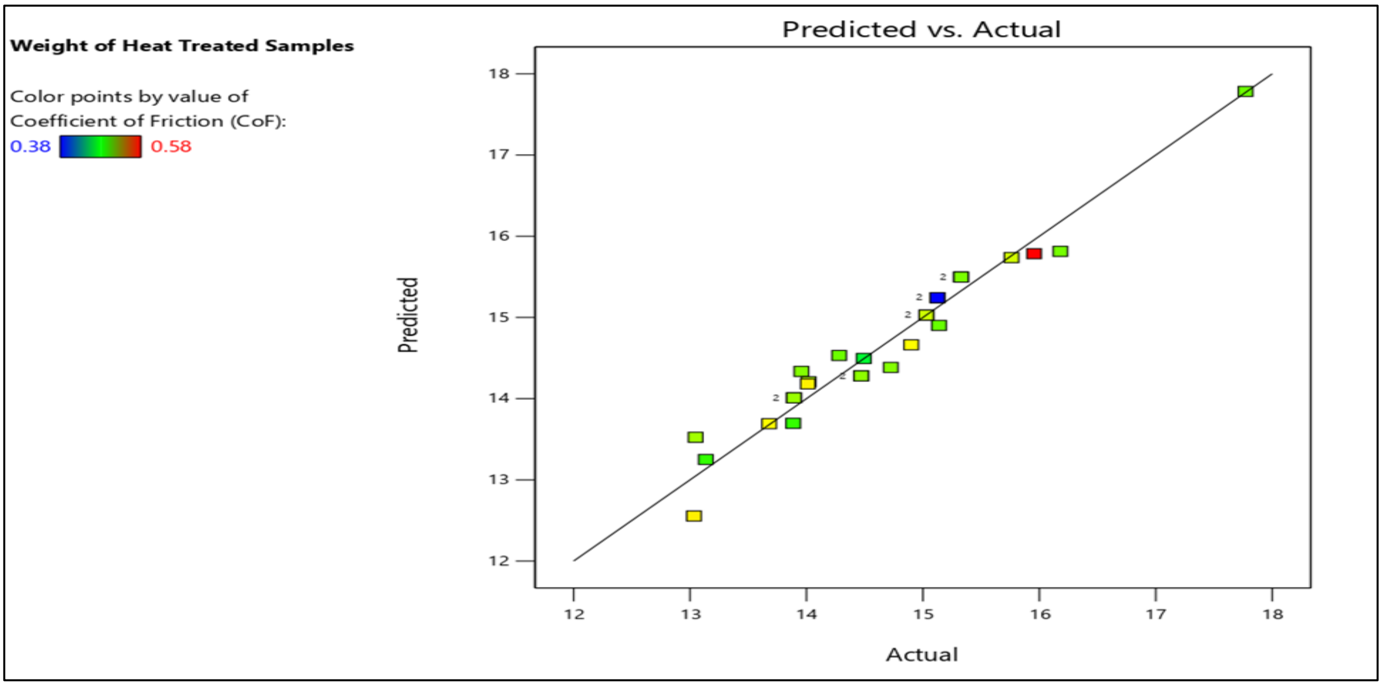


Fig 9: Showing the Predicted and Actual Values for the Weight of Heat

- *Effect of the Additives on the Response*

The result generated shows the contour diagram of the relationship between the temperature and the factor of variables considered i.e. wear rate, corrosion rate, Coefficient of Friction, and weight of heat treatment.

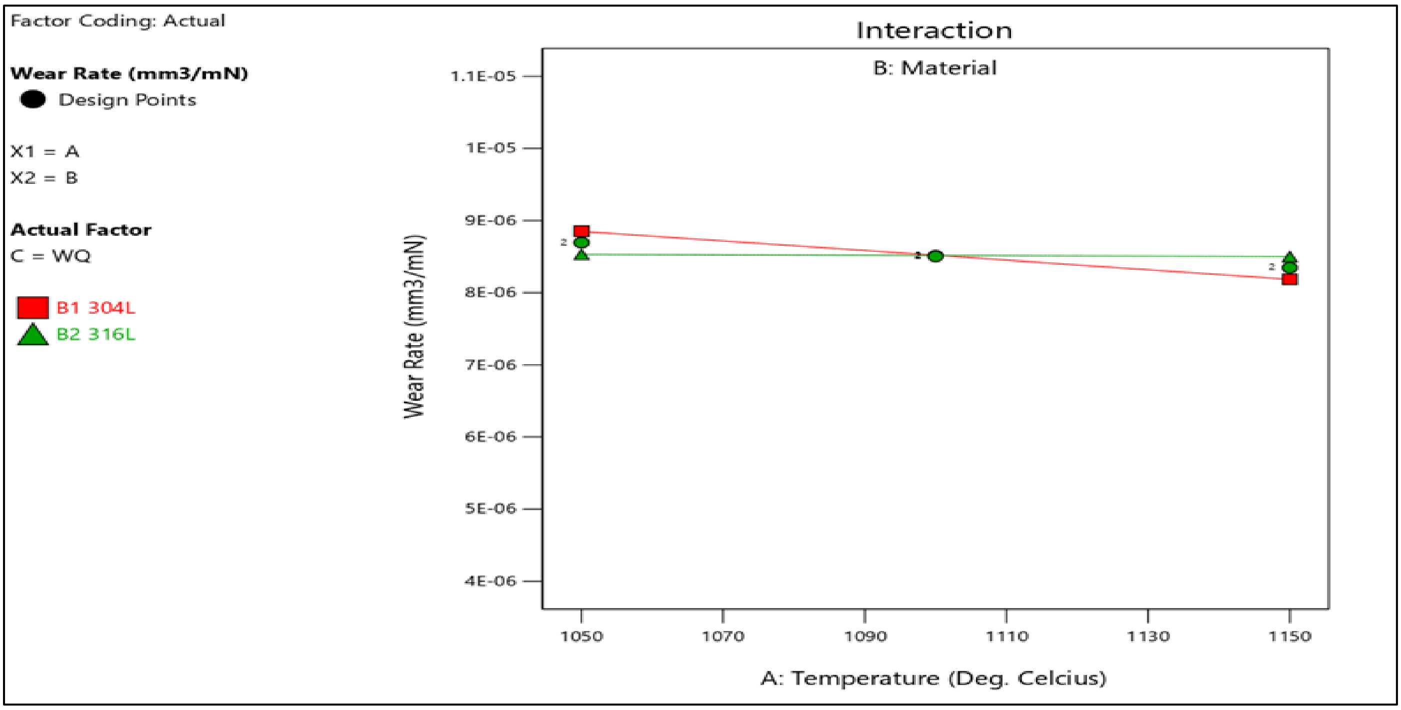


Fig 10: Diagram Showing the Interaction Between the Variables and the Wear Rate

The diagram illustrating the correlation between temperature in degrees Celsius and the material wear rate revealed an intersection at 1100 degrees. The materials in question, namely B1 304L and B2 316L, exhibited distinct behavior at this temperature. Specifically, the wear rate of B1 (304L) experienced a decrease following the interaction, in contrast to the behavior observed in 316L. These observations were made under the specific conditions of water quench (WQ).

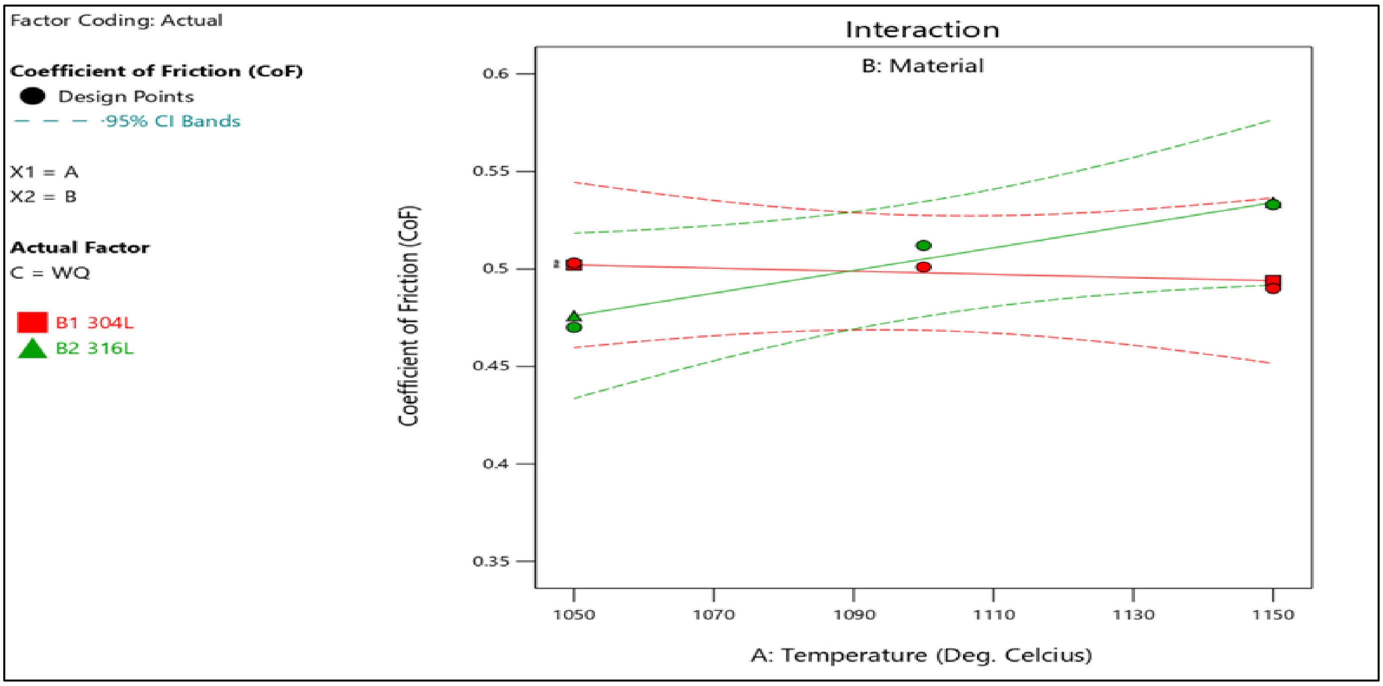


Fig 11: Diagram Showing the Interaction Between the Variables and the Coefficient of Friction (CoF)

The diagram illustrating the correlation between temperature in degrees Celsius and its effect on the material's coefficient of friction revealed a significant intersection at a temperature of 1090 degrees with a coefficient close to 0.5. The materials under examination, namely B1 304L and B2 316L, displayed distinct behavior at this intersection point. Specifically, the coefficient of friction for B1 material (304L) experienced a decrease following the interaction, whereas the coefficient for B2 material (316L) exhibited an opposing trend. These observations were made under the specific conditions of water quench (WQ).

ISSN No:-2456-2165 https://doi.org/10.38124/ijisrt/IJISRT24OCT336

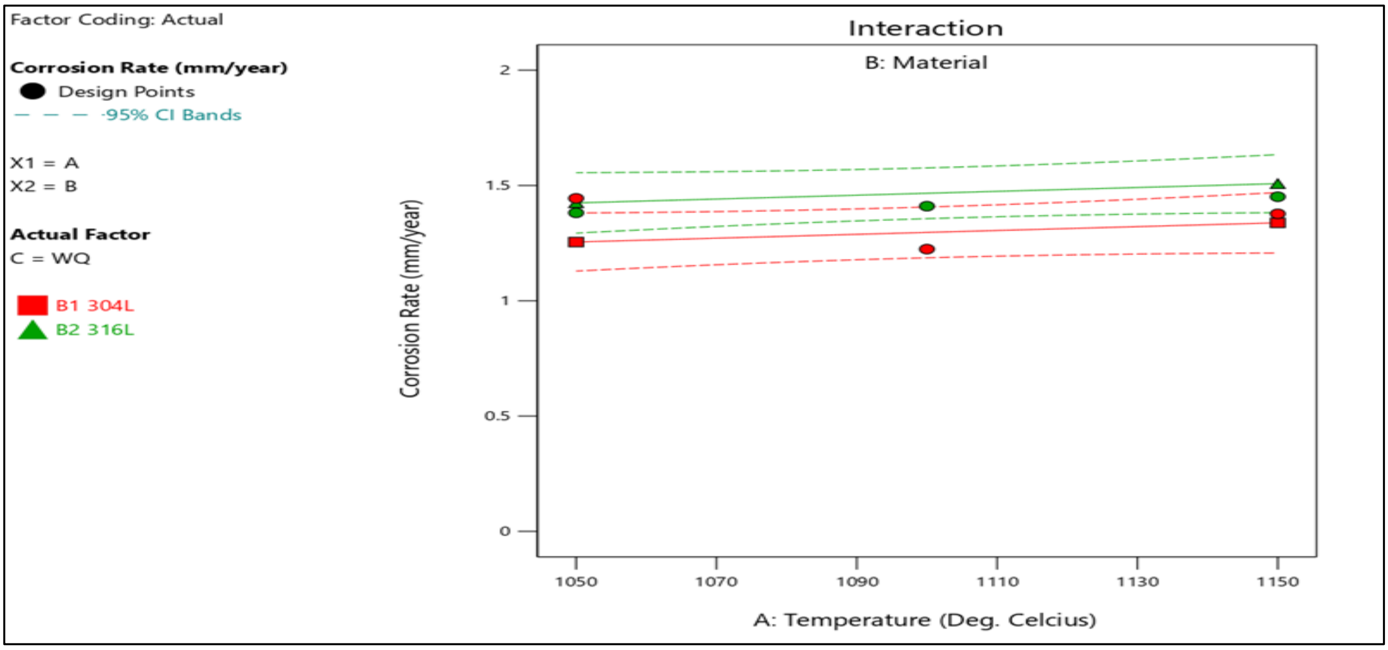

Fig 12: Diagram Showing the Interaction Between the Variables and the Corrosion Rate

The diagram illustrating the correlation between temperature in degrees Celsius and its impact on the material's corrosion rate revealed a consistent trend: the yield varied in tandem with temperature changes, mirroring the behavior of the corrosion rate. Interestingly, irrespective of the corrosion presence, elevating the temperature consistently led to an increase in yield by a uniform degree. These findings were based on observations conducted under the specific condition of water quench (WQ) and involved materials 304L and 316L.

## V. CONCLUSION

This research focuses on controlling weld decay in AISI 304L/316L alloy weldments in cryogenic environments like liquefied natural gas (LNG). The Tungsten Inert Gas (TIG) welding technique was used, followed by thermokinetic treatment at temperatures of 1050°C, 1100°C, and 1150°C, and cooling in five mediums (Water, Salt, Air, Salt quenched with annealing, and Water quenched with annealing). Key findings include:

- Optical microscopy analysis showed that air-cooled samples had smoother bonding, while water-quenched samples with annealing lacked significant bonding effects.
- SEM analysis revealed coarse surfaces with uneven particle distribution. The predominant elements detected in the sample were Iron (Fe), Chromium (Cr), and Nickel (Ni) at intensities of 34 Cps/eV, 16 Cps/eV, and 9 Cps/eV respectively. The Energy Dispersive X-ray Spectroscopy (EDS) analysis summarized the elements identified in each sample.
- Corrosion analysis showed wave-like potential changes, while wear and coefficient of friction studies highlighted the importance of lower friction in enhancing wear resistance.
- A temperature-corrosion rate relationship indicated that higher temperatures increased yield and corrosion rates, especially with water quenching.
- Response Surface Methodology (RSM) identified optimal conditions for temperature (1112.68°C), material (316L), and quenching medium (Salt quenched with annealing), improving wear, corrosion resistance, and sample weight.

➢ *Recommendations*

Based on the findings and conclusions of this research, the following recommendations are being made. Future researchers should;

- **Explore a Broader Range of Heat Treatment Temperatures:** Instead of restricting the study to only three specific heat treatment temperatures, future research should include a wider range of temperatures. This approach will provide a more comprehensive understanding of how different heat treatments impact the properties of the materials.
- **Encourage Further Research:** Continued investigation is necessary, focusing on new variables and approaches, including long-term durability, environmental impact, and cost-effectiveness.
- **Recommend Nanoindentation for Detailed Mechanical Property Analysis:** For accurate assessment of mechanical characteristics at the nanoscale, such as hardness and elastic modulus, using nanoindentation techniques is advised. This can provide valuable information about the behaviour of materials and microstructural changes that occur during processing.
- **Expand the Use of Diverse Welding Processes:** Future research should include various welding techniques like Gas Metal Arc Welding (GMAW), Flux-Cored Arc Welding (FCAW), and Submerged Arc Welding (SAW) to identify the most effective methods for achieving optimal weld quality and performance.

## REFERENCES

[1]. P. A. Schweitzer, "Fundamentals of corrosion: mechanisms, causes, and preventative methods," CRC Press, 2003. Accessed: Oct. 04, 2024. [Online]. Available: https://digital.library.tu.ac.th/tu_dc/frontend/Info/item/dc:10589

[2]. L. L. Shreir, *Corrosion: metal/environment reactions*. Newnes, 2013.

[3]. C. E. Butzke, *Winemaking problems solved*. Elsevier, 2010.

[4]. H. Shaikh *et al.*, "Use of eddy current testing method in detection and evaluation of sensitisation and intergranular corrosion in austenitic stainless steels," *Corros. Sci.*, vol. 48, no. 6, pp. 1462–1482, 2006.

[5]. R. Singh, S. G. Chowdhury, B. R. Kumar, S. K. Das, P. K. De, and I. Chattoraj, "The importance of grain size relative to grain boundary character on the sensitization of metastable austenitic stainless steel," *Scr. Mater.*, vol. 57, no. 3, pp. 185–188, 2007.

[6]. W. Yan, W. Wang, Y. Shan, K. Yang, and W. Sha, *9-12Cr Heat-Resistant Steels*. in Engineering Materials. Cham: Springer International Publishing, 2015. doi: 10.1007/978-3-319-14839-7.

[7]. F. Peter Ford, B. M. Gordon, and R. M. Horn, "Corrosion in boiling water reactors," 2006, Accessed: Oct. 04, 2024. [Online]. Available: https://dl.asminternational.org/handbooks/edited-volume/26/chapter/352984/Corrosion-in-Boiling-Water-Reactors

[8]. S. V. Pawar, "Fabrication of precipitation-hardened aluminum microchannel cooling plates for adsorption-based hydrogen storage systems," 2013, Accessed: Oct. 04, 2024. [Online]. Available: https://ir.library.oregonstate.edu/concern/graduate_thesis_or_dissertations/xs55mg19f

[9]. J. C. Lippold, *Welding metallurgy and weldability*. John Wiley & Sons, 2014. Accessed: Oct. 04, 2024. [Online]. Available: https://books.google.com/books?hl=en&lr=&id=EldwBQAAQBAJ&oi=fnd&pg=PP13&dq=Lippold,+John.+(2016).+Welding+Metallurgy+and+Weldability%E2%80%94John+C.+Lippold%E2%80%94Google+Books.&ots=Z2DaLQrbJp&sig=brpqRpxsh6zMHJmIWGIgPHmCjJI

[10]. N. Parvathavarthini and R. K. Dayal, "Influence of chemical composition, prior deformation and prolonged thermal aging on the sensitization characteristics of austenitic stainless steels," *J. Nucl. Mater.*, vol. 305, no. 2–3, pp. 209–219, 2002.

[11]. Y. Nam and S. K. Hong, "Force control system design for aerodynamic load simulator," *Control Eng. Pract.*, vol. 10, no. 5, pp. 549–558, 2002.

[12]. E. A. Trillo and E. A. Trillo, "A TEM investigation of M23C6 carbide precipitation behaviour on varying grain boundary misorientations in 304 stainless steels," *J. Mater. Sci.*, vol. 33, no. 5, pp. 1263–1271, Mar. 1998, doi: 10.1023/A:1004390029071.

[13]. H. Kokawa, M. Shimada, M. Michiuchi, Z. J. Wang, and Y. S. Sato, "Arrest of weld-decay in 304 austenitic stainless steel by twin-induced grain boundary engineering," *Acta Mater.*, vol. 55, no. 16, pp. 5401–5407, 2007.

[14]. T. Kvackaj *et al.*, "Influence of Processing Conditions on Properties of AISI 316LN Steel Grade," *J. Mater. Eng. Perform.*, vol. 29, no. 3, pp. 1509–1514, Mar. 2020, doi: 10.1007/s11665-020-04561-y.

[15]. Z. Chen *et al.*, "Three-dimensional network space Ag3PO4/NP-CQDs/rGH for enhanced organic pollutant photodegradation: synergetic photocatalysis activity/stability and effect of real water quality parameters," *Chem. Eng. J.*, vol. 390, p. 124454, 2020.

[16]. M. Vasudevan, A. K. Bhaduri, B. Raj, and K. P. Rao, "Delta ferrite prediction in stainless steel welds using neural network analysis and comparison with other prediction methods," *J. Mater. Process. Technol.*, vol. 142, no. 1, pp. 20–28, 2003.

[17]. A. S. Lima, A. M. Nascimento, H. F. G. Abreu, and P. De Lima-Neto, "Sensitization evaluation of the austenitic stainless steel AISI 304L, 316L, 321 and 347," *J. Mater. Sci.*, vol. 40, no. 1, pp. 139–144, Jan. 2005, doi: 10.1007/s10853-005-5699-9.

[18]. J. Xie, H. Li, C. Li, J. Zhang, and M. Luo, "Review on occupant-centric thermal comfort sensing, predicting, and controlling," *Energy Build.*, vol. 226, p. 110392, 2020.

[19]. S. S. M. Tavares, J. M. Pardal, E. Ponzio, A. Loureiro, and J. A. De Souza, "Influence of microstructure on the corrosion resistance of hyperduplex stainless steel," *Mater. Corros.*, vol. 61, no. 4, pp. 313–317, Apr. 2010, doi: 10.1002/maco.200905386.